IRAP – December 8, 2025

Presented by

Case 1: Drs. Deven Gupta and Aliya Husain

Diagnosis: Usual interstitial pneumonia (UIP), Nonspecific interstitial pneumonia (NSIP), and pulmonary alveolar proteinosis (PAP) on bilateral lung explants.

Clinical history: The patient is a 37-year-old African American female with a history of childhood asthma in her 20's. She endorsed a history of dust and fume exposure related to occupational work for a few years. She denies a history of smoking, illicit drug use, mold or pet exposure. At 30, the patient endorsed episodic diffuse muscle pain, weakness limiting and polyarthralgia's. She was treated with methotrexate with minimal improvement. Serologies at an outside hospital were positive for ANA, RNP, anti-smith, PL-12. Over the next 4 years, she had interval follow up with continued worsening of symptoms.

At 34, the patient began to have a significant decline in breathing requiring her to quit work. A CT-chest was performed and showed peripheral honeycombing, traction bronchiectasis, and ground glass opacities, greatest in the lower lung zones. She was diagnosed with mixed connective tissue disease associated interstitial lung disease (MCTD-ILD) and treated with multiple immunosuppressive agents and supplemental home oxygen.

Between 35 and 36, the patient had over 7 hospitalizations, mostly secondary to volume overload in the setting of significant pulmonary hypertension and RV failure. At 37, she was listed for a bilateral sequential lung transplant. The patient ultimately received a bilateral lung transplant with surgical pathology evaluation of bilateral lung explants.

Gross Findings (on explanted lungs): Variable pathologies including pale to tan dense fibrosis (LUL) as well as peripheral honeycombing (LLL). Right lung similarly shows pale to tan dense fibrosis which is worse in the lower lobe.

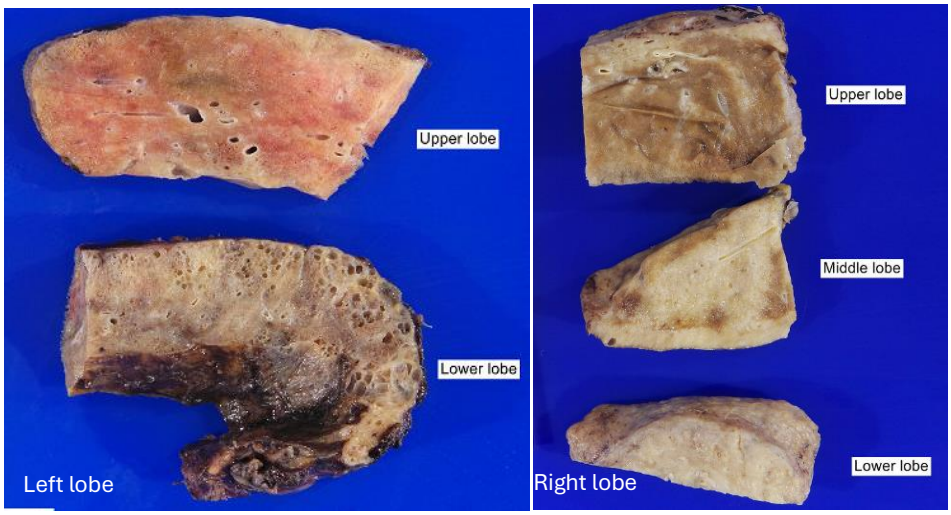

Microscopic findings (on explanted lungs): Dense patchy fibrosis replacing the alveolar architecture, proliferation of spindle cells adjacent to the alveoli within a gray matrix, and residual airspaces lined by bronchial epithelium (RLL, top 2 panels). Dense homogenous thickening of the alveolar septa with preservation of the lung architecture (RUL, bottom left panel). Finely granular pink proteinaceous material within the alveoli (bilaterally, bottom right panel).

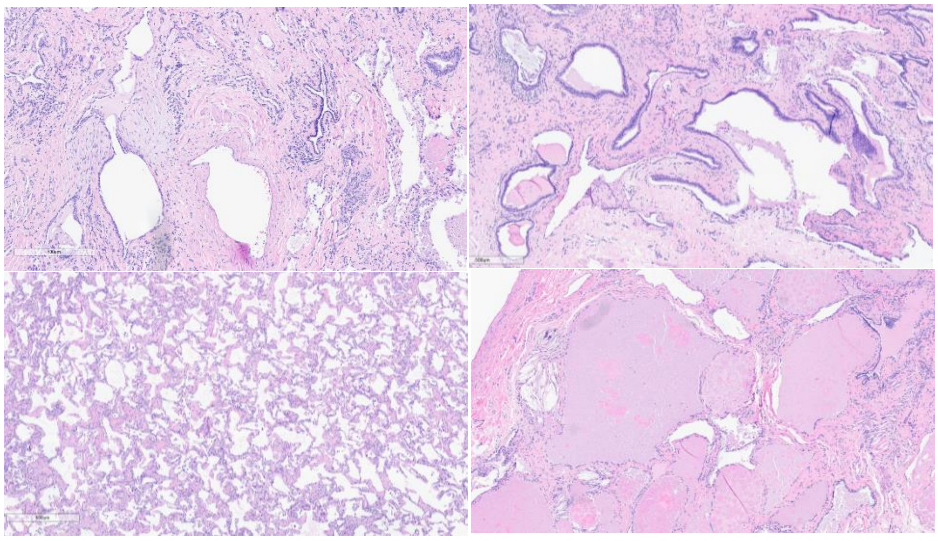

Differential Diagnosis:

- Usual interstitial pneumonia (UIP)
- Diffuse alveolar damage (DAD)
- Hypersensitivity pneumonitis
- Nonspecific interstitial pneumonia (NSIP)
- Mucous plugging
- Pulmonary alveolar proteinosis (PAP)
- Pulmonary edema
- Intra alveolar fibrin

Further work-up: Examination of the right lower lobe revealed spatial heterogeneity, fibroblastic foci and honeycombing, consistent with a UIP pattern. The right upper lobe showed preservation of lung architecture with temporal homogeneity, consistent with an NSIP pattern. Immunohistochemical analysis of the finely granular, pink proteinaceous material was performed. It demonstrated this material to be positive for both PAS-D and Napsin-A, consistent with PAP.

Discussion: This case of bilateral lung explants demonstrates three different patterns including UIP, NSIP and PAP, highlighting the importance of "staying curious." Importantly, a mixed pattern of UIP and NSIP is often seen in patients with mixed connective tissue diseases (MCTD). However, PAP is not. PAP is characterized by the accumulation of surfactant within alveoli secondary to impaired clearance by alveolar macrophages. There are three types of PAP: autoimmune, congenital and secondary.

The diagnosis of PAP can often be mistaken for certain mimickers including intra-alveolar fibrin, mucous plugging and pulmonary edema. However, these entities won't appear as finely granular or pink/proteinaceous as classic PAP. In difficult cases, IHC stains can be very helpful. Along with PAS-D, a recent paper has shown Napsin-A to be highly specific for PAP.

Due to our patient having diffuse evidence of PAP we investigated why. The literature showed rare case reports demonstrating PAP secondary to immunosuppression. To further characterize this, we examined 22 cases of patients with bilateral lung explants who had evidence of UIP. Out of these 22 patients, 10 had histories of CTD and had been on pretransplant immunosuppression for 53.1 months on average. However, our patient was the only one to show definitive and diffuse evidence of PAP. Importantly, 3 patients, including those with and without CTD, had evidence of PAP-like material. This material didn't appear like classic PAP on morphology as it was only focal, didn't appear as bright pink/proteinaceous and didn't expand the alveoli.

Overall, this case was meant to highlight the importance of not stopping after the first diagnosis, considering PAP on the differential for unexplained respiratory distress, the utility of PAS-D and Napsin-A for diagnosis and watching for PAP-like material/PAP mimickers.

References:

1. Carrington JM, Hershberger DM. Pulmonary Alveolar Proteinosis. [Updated 2023 Jul 25]. In: StatPearls [Internet]. Treasure Island (FL): StatPearls Publishing; 2025 Jan-. Available from: https://www.ncbi.nlm.nih.gov/books/NBK482308/
2. Catherine Larose, Charles Leduc, Martin Chevrier; Napsin-A Immunohistochemistry in the Diagnosis of Pulmonary Alveolar Proteinosis. Arch Pathol Lab Med 1 June 2025; 149 (6): 568–572. doi: https://doi.org/10.5858/arpa.2024-0136-OA
3. Hammami S, Harrathi K, Lajmi K, Hadded S, Ben Meriem C, Guédiche MN. Congenital pulmonary alveolar proteinosis. Case Rep Pediatr. 2013;2013:764216. doi: 10.1155/2013/764216. Epub 2013 Apr 27. PMID: 23710403; PMCID: PMC3655498.

4. Larose C, Leduc C, Chevrier M. Napsin-A Immunohistochemistry in the Diagnosis of Pulmonary Alveolar Proteinosis. Arch Pathol Lab Med. 2025 Jun 1;149(6):568-572. doi: 10.5858/arpa.2024-0136-OA. PMID: 39370148.
5. Lawrence M. Nogee, Interstitial lung disease in newborns, Seminars in Fetal and Neonatal Medicine, Volume 22, Issue 4, 2017, Pages 227-233, ISSN 1744-165X, https://doi.org/10.1016/j.siny.2017.03.003.
6. McCarthy C, Carey BC, Trapnell BC. Autoimmune Pulmonary Alveolar Proteinosis. Am J Respir Crit Care Med. 2022 May 1;205(9):1016-1035. doi: 10.1164/rccm.202112-2742SO. PMID: 35227171; PMCID: PMC9851473.
7. Yanagisawa A, Konaka H, Tanaka M, Ihara S, Tachibana I. Pulmonary Alveolar Proteinosis During Intensive Immunosuppressive Treatment for Acute Exacerbation of Interstitial Pneumonia: A Case Report and Literature Review. Cureus. 2024 Nov 28;16(11):e74669. doi: 10.7759/cureus.74669. PMID: 39734970; PMCID: PMC11681919.
8. Zhang D, Tian X, Feng R, Guo X, Wang P, Situ Y, Xiao Y, Xu KF. Secondary pulmonary alveolar proteinosis: a single-center retrospective study (a case series and literature review). BMC Pulm Med. 2018 Jan 25;18(1):15. doi: 10.1186/s12890-018-0590-z. PMID: 29368649; PMCID: PMC5784666.

Case 2: Drs. Dane Wuori and Neval Ozkaya

Diagnosis: Systemic EBV-positive T-cell lymphoma of childhood with associated EBV-positive Hodgkin-like infiltrate

Clinical history:

The patient is a 14-year-old male with no significant past medical history who transferred to UChicago from an outside hospital for evaluation of a new mediastinal mass detected on imaging. Recently, he endorsed symptoms of nausea, emesis, diarrhea, and intermittent fevers. He has not had any respiratory or urinary symptoms. In addition to the fevers, he has had significant, unintentional weight loss of approximately 20 lbs. from 135 to 115 lbs. A PET/CT scan showed diffuse, bulky lymphadenopathy extending from the neck to the pelvis which specifically involved the spleen, bones, and Waldeyer's ring. He underwent excisional lymph node biopsy of the left groin.

Morphology:

Morphology at low power for the excised lymph node is notable for a diffusely effaced architecture with limited normal lymph node architecture remaining. At high power, there is a prominent infiltrate of large, pleomorphic cells with prominent nucleoli, pale cytoplasm that are reminiscent of Hodgkin cells admixed a polymorphous lymphoplasmacytic infiltrate.

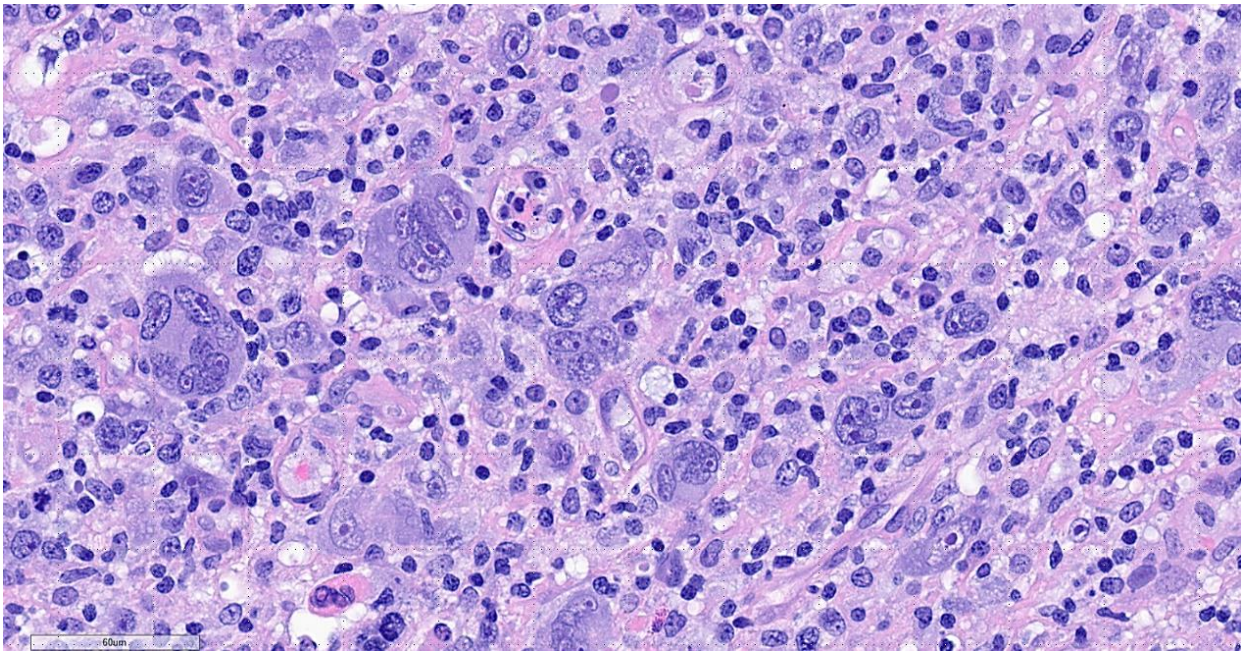

Differential diagnosis:

Classic Hodgkin Lymphoma

Mediastinal gray zone lymphoma

Anaplastic large cell lymphoma

EBV associated diffuse large B-cell lymphoma

Stains:

The Hodgkin-like cells stain positive for CD30, variable CD15, dim PAX5, negative CD20 and CD3. EBER is positive in Hodgkin-like cells and also in the background lymphocytes. CD3/EBER double stain is positive. The T-cell infiltrate has CD5 aberrant loss. CD4 highlights background histiocytes. CD8 positive T-cells are Beta F1 and cytotoxic T-cell marker positive. CD5 shows aberrant T-cell loss of staining. CD3 at closer inspection shows cytological atypia and larger cell sizes.

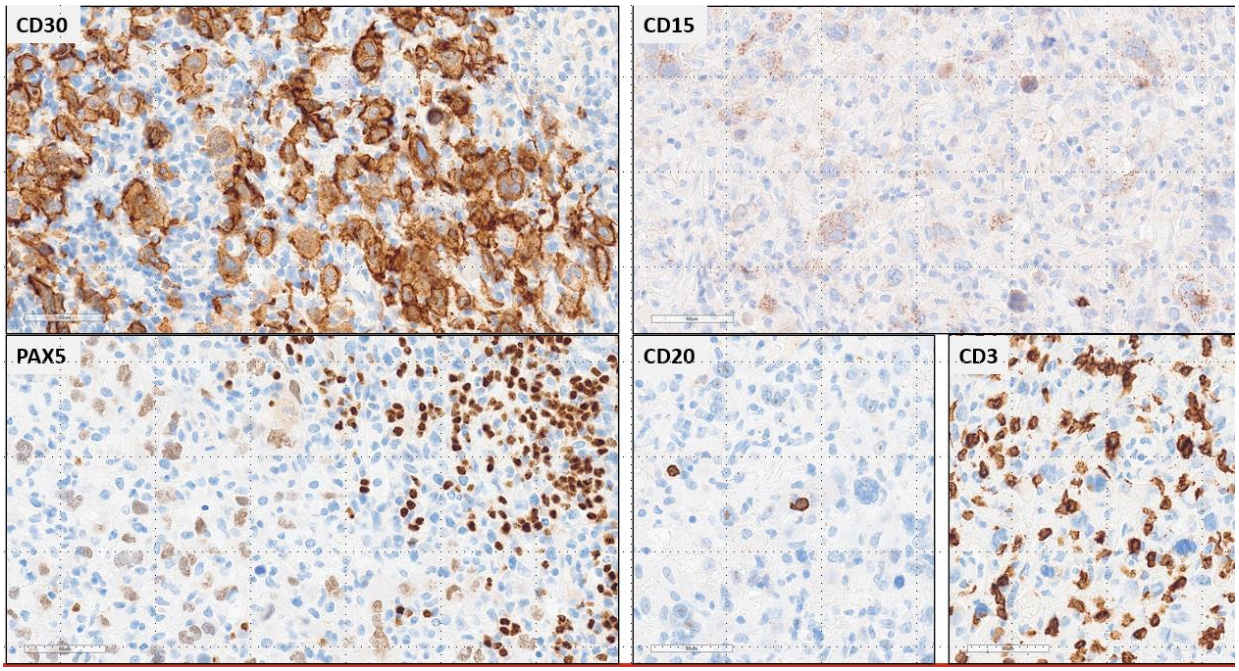
CD30
CD15
PAX5
CD20
CD3

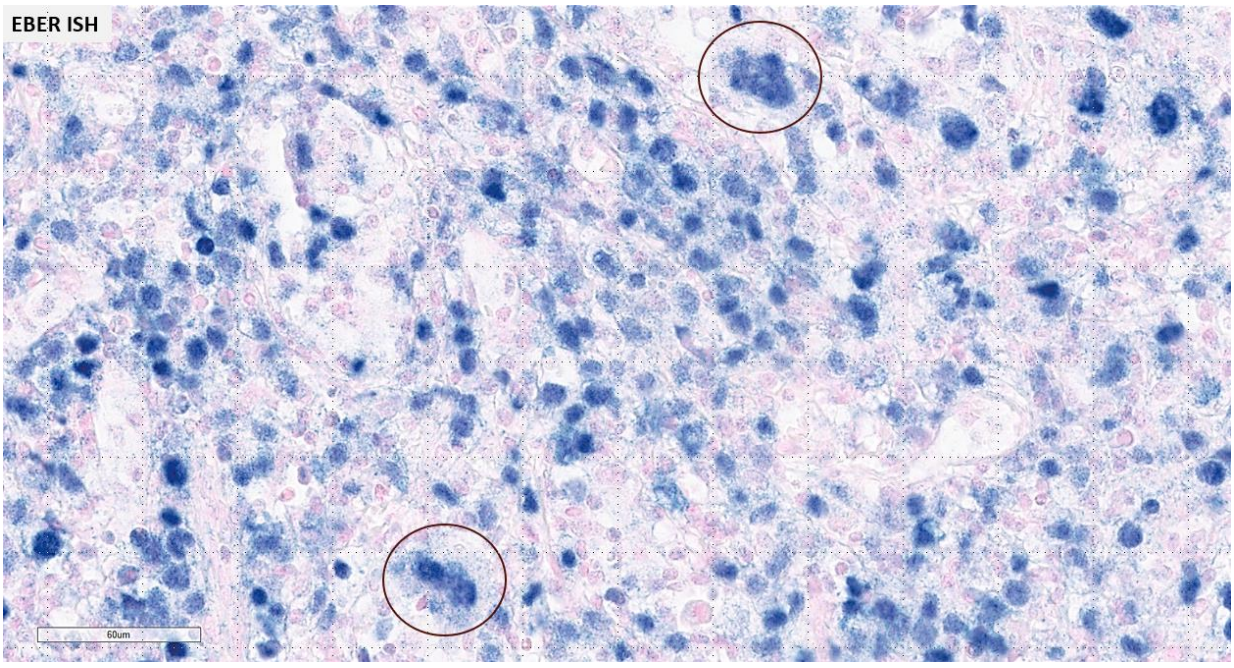
EBER ISH
60um

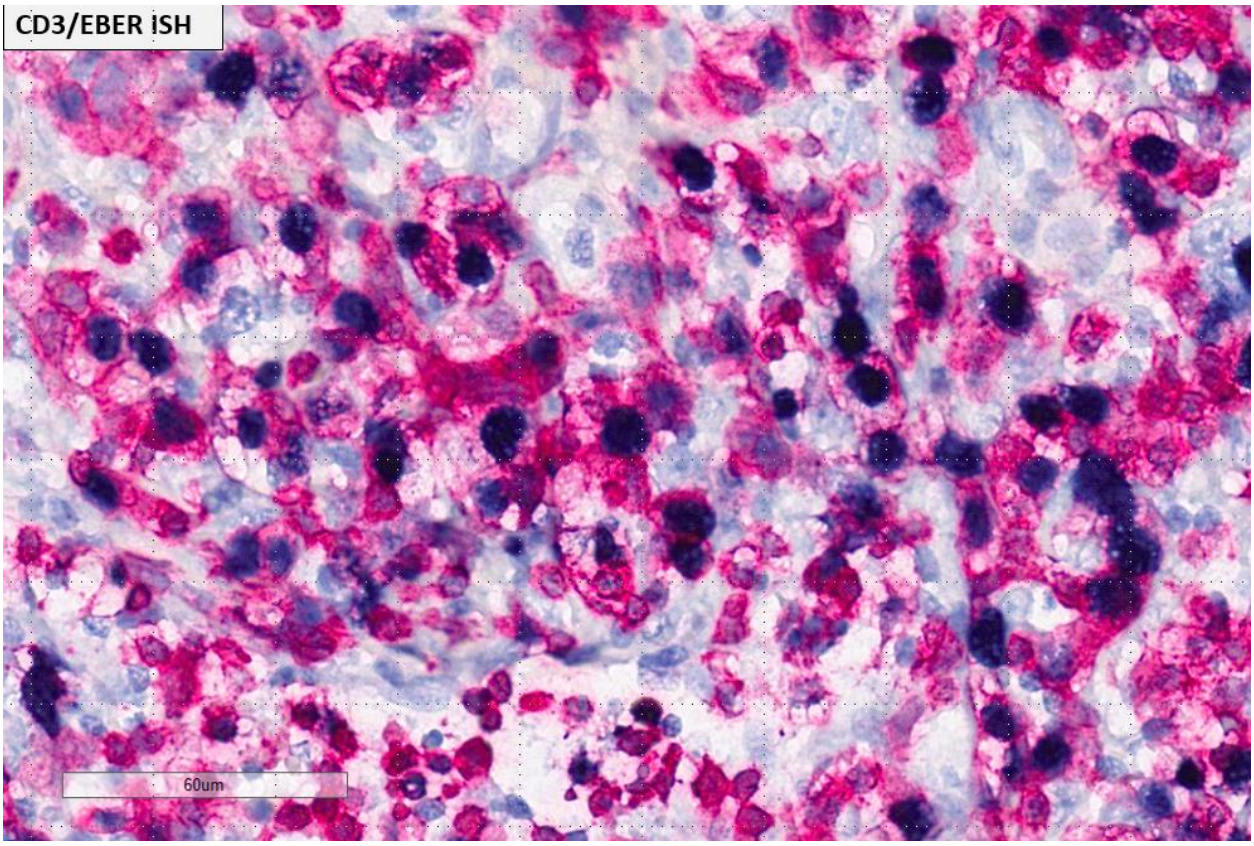

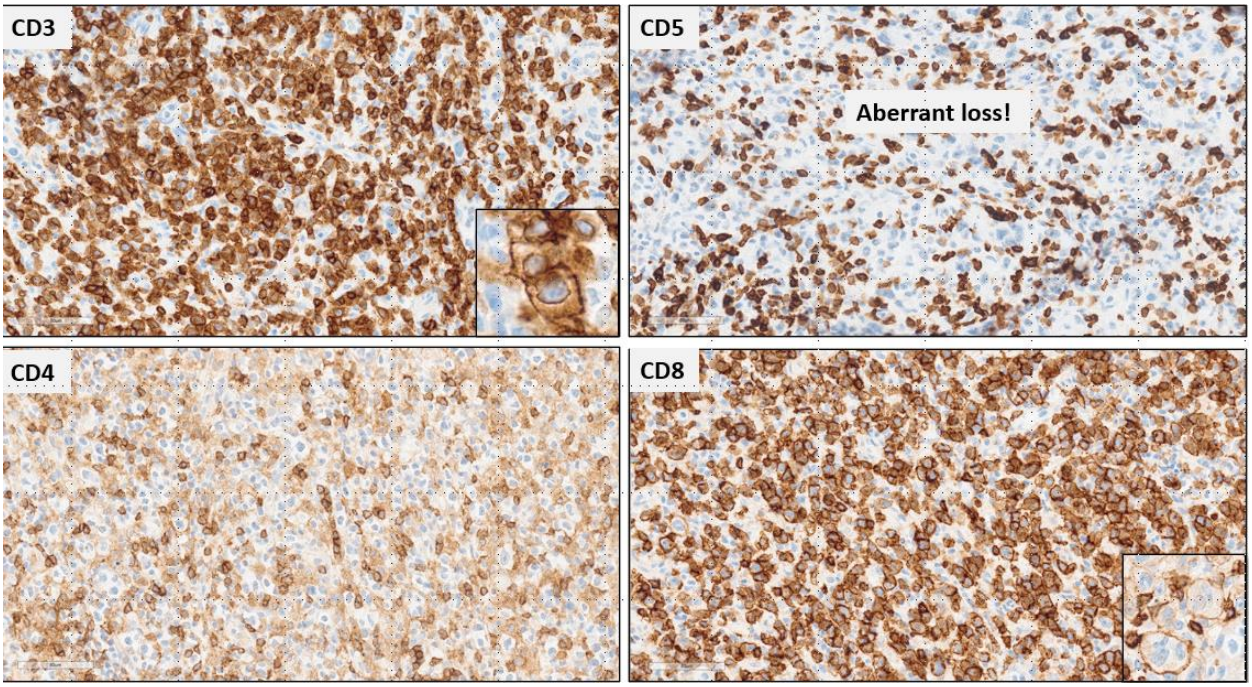

Molecular:

Molecular is positive for TCR beta/gamma clonality

B cells are polyclonal

PD-L1 amplification and point mutation

Complex karyotype

Discussion:

We identified an aberrant EBV-positive, CD8-positive cytotoxic T-cell infiltrate involving both lymph node and bone marrow. These cells show cytologic atypia, architectural effacement (especially in the lymph node), aberrant immunophenotype, and importantly, a clonal T-cell population by PCR, supporting a true EBV-driven T-cell lymphoproliferative disorder rather than a reactive process. EBV-infected T or NK cells are inherently abnormal. They do not occur in benign EBV infections, so their presence automatically points to a pathologic EBV-driven T-cell process. There was also a diagnostic pitfall of a second component seen: EBV-positive Hodgkin-like large cells within the lymph node. These cells show a CHL-like phenotype but with aberrant CD8 and cytotoxic marker expression, which is unusual for classic Hodgkin lymphoma. PCR studies confirmed no clonal B-cell population, arguing against a distinct EBV-positive B-cell lymphoma process. And it is already known that these Hodgkin-like cells can occasionally be seen in the background of T-LPDs or T-cell lymphomas, likely due to loss of T-cell immune control, leading to secondary EBV-driven B-cell expansion. So overall, the findings support a primary EBV-positive cytotoxic T-cell process, with secondary EBV-positive Hodgkin-like B-cells.

Take home points:

If you see Hodgkin like cells, the diagnosis is not CHL without IHC proof and strong clinical findings supporting it

Classic Hodgkin Lymphoma has characteristic findings of contiguous spread with rare extranodal involvement, and if you have extranodal disease consider other diagnoses

T-cells or NK cells that are infected with EBV is pathologic and should be worked up

Pay attention to what EBV is staining

References:

1. Alaggio, Rita et al. “The 5th edition of the World Health Organization Classification of Haematolymphoid Tumours: Lymphoid Neoplasms.” *Leukemia* vol. 36,7 (2022): 1720-1748. doi:10.1038/s41375-022-01620-2
2. *CAEBV of T/NK-Cell Type Mimicking Classic Hodgkin Lymphoma, Am J. Surg Pathol., 2019*

3. El-Mallawany, Nader Kim et al. “Haemophagocytic lymphohistiocytosis and Epstein-Barr virus: a complex relationship with diverse origins, expression and outcomes.” *British journal of haematology* vol. 196,1 (2022): 31-44. doi:10.1111/bjh.1763

Case 3: Drs. Priscilla Natcher, Tatjana Antic, and Nicole Cipriani

Final Diagnosis on Cytopathology: Basaloid Salivary Gland Neoplasm

Final Diagnosis on Surgical Pathology: *HMGA2::WIF1*-associated monophasic salivary neoplasm

Clinical History: The patient is a 58-year-old with no significant past medical history presenting with a right parotid mass. He first noticed it three months ago after he intentionally lost some weight. On review of old photos, he thinks it may have been there longer. The patient denies pain, facial weakness/paralysis, otalgia, dysphagia, odynophagia, voice changes, breathing difficulty, cough, hemoptysis, and unintended weight loss. He has a history of cigarette smoking but quit 18 years ago and is a daily marijuana smoker. No history of head and neck cancer. No history of head and neck surgery. On soft tissue CT imaging, a hypodense heterogeneously enhancing oval-shaped well-circumscribed lesion within the right parotid gland, measuring 2.8 x 2.1 x 2.6 cm, was noted. His head and neck soft tissue ultrasound showed predominantly hypoechoic lesion with internal vasculature is noted measuring 3 x 2 x 2.6 cm, likely within the parotid gland. He has not noticed any growth of the mass in the following two months after the initial onset. He underwent an FNA and is now scheduled for a right parotidectomy. The FNA slide is submitted for review.

FNA slides:

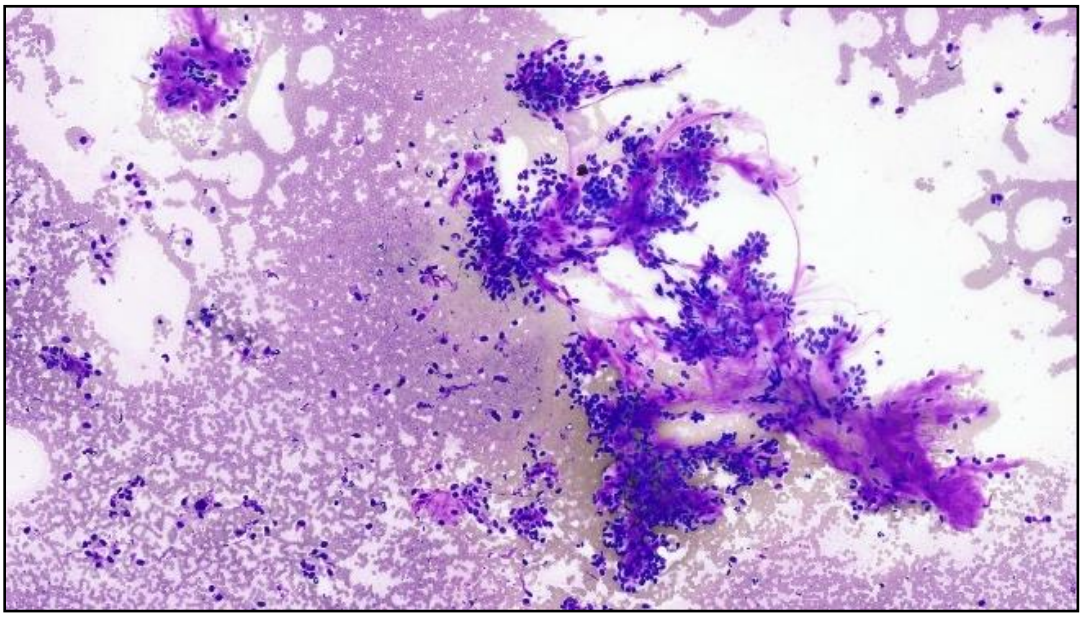

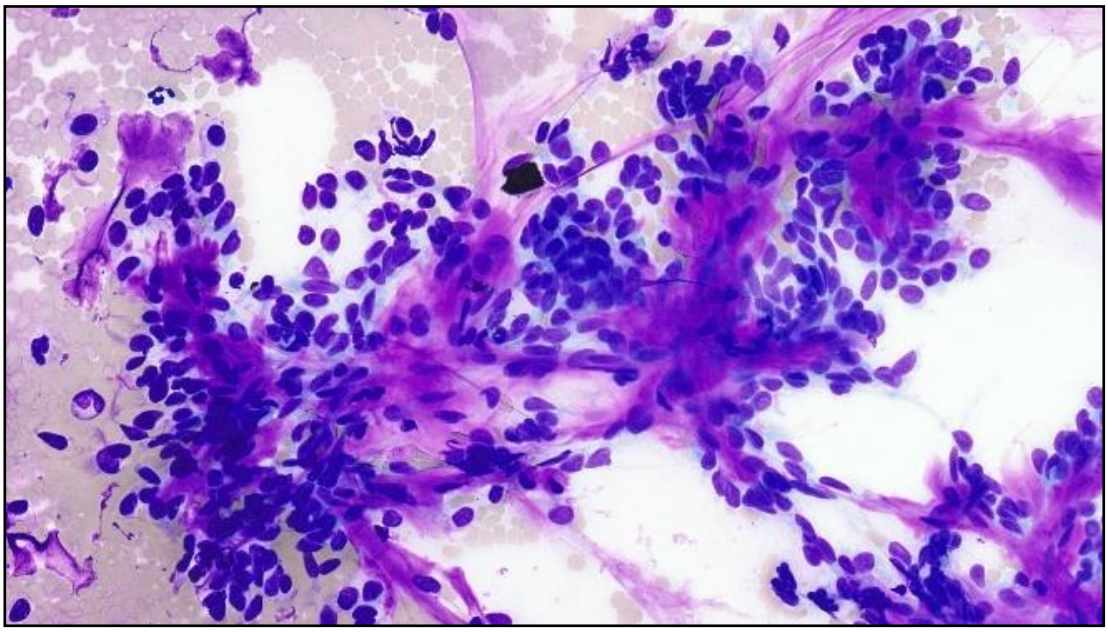

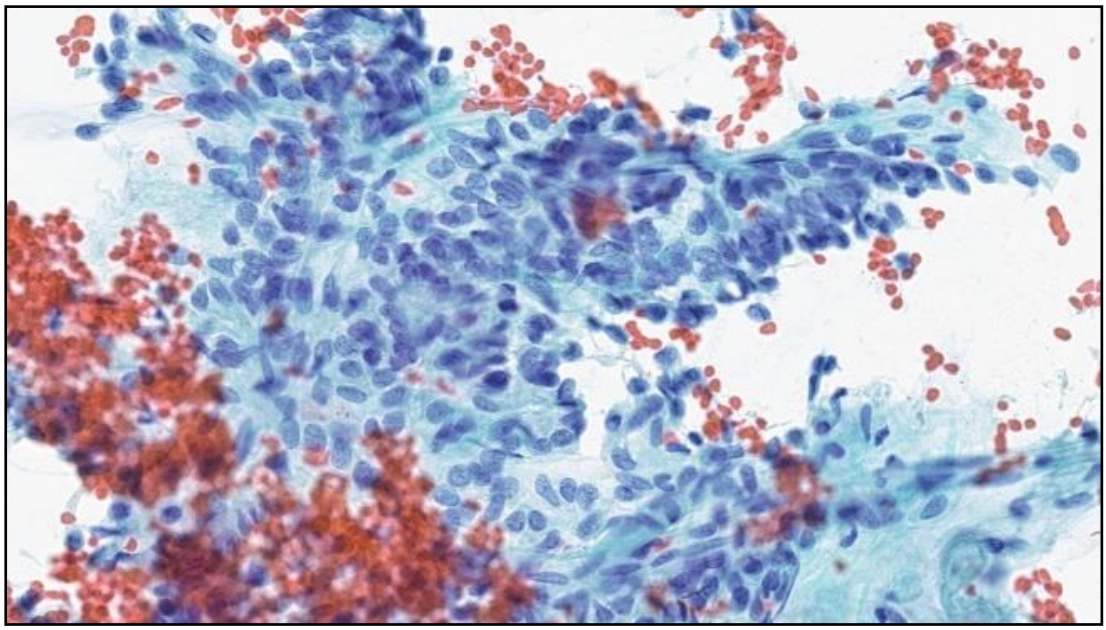

Gross Findings (on resection specimen):

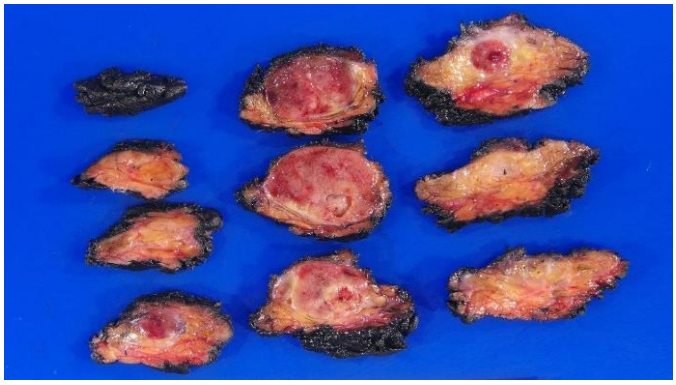

Microscopic Findings (on resection specimen):

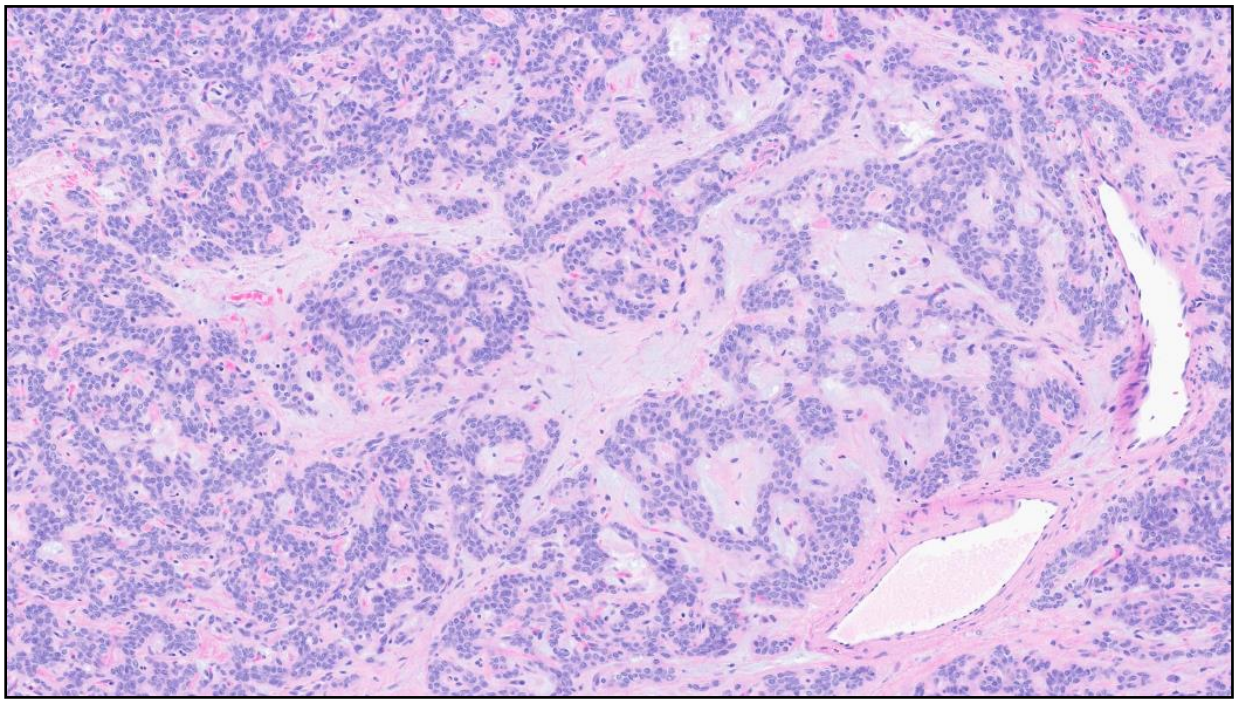

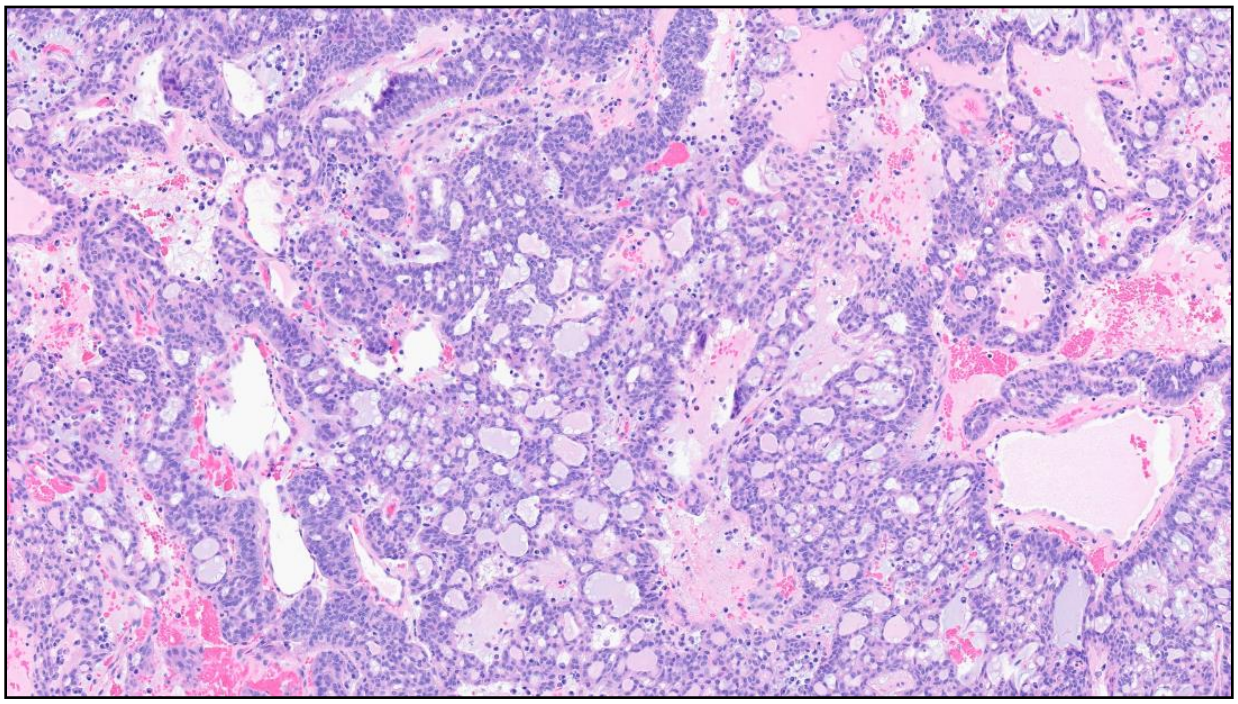

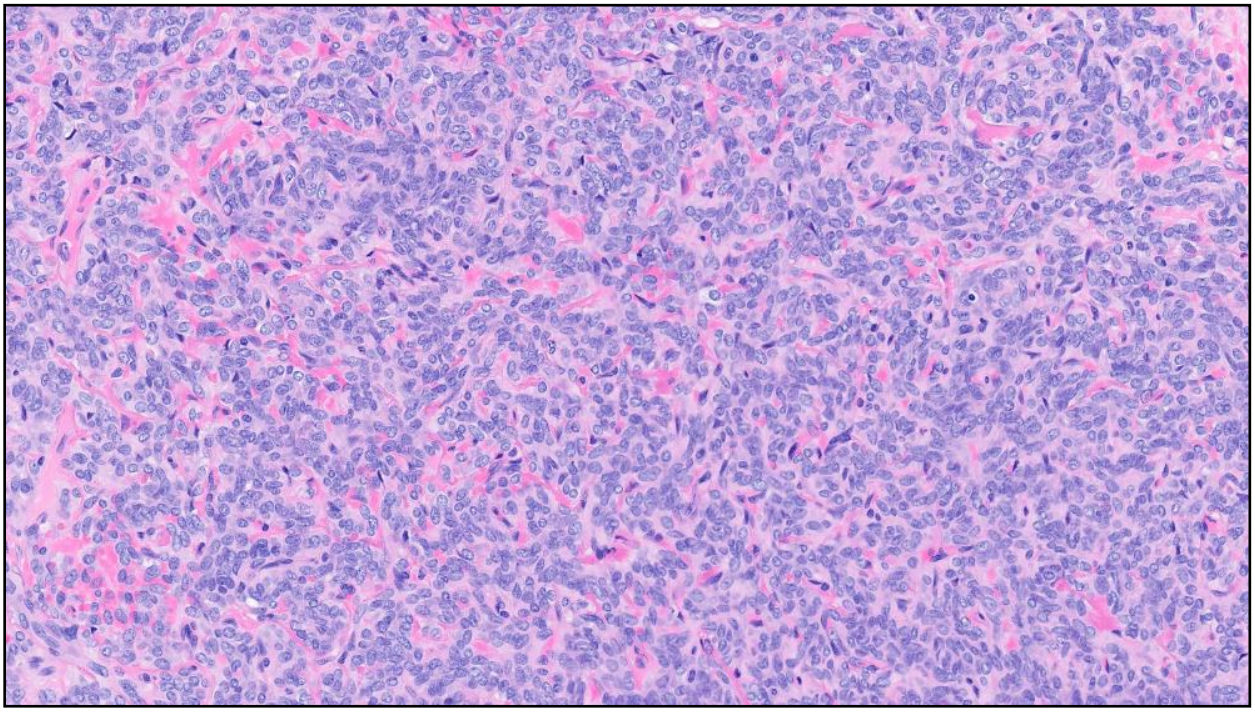

The tumor is well-circumscribed and composed of trabeculae, cords, and microcysts within a myxoid to vascular stroma. There is no evidence of infiltrative growth or high grade features. Therefore, behavior is expected to mirror that of adenoma.

Differential Diagnosis:

- Basal cell adenoma
- Pleomorphic adenoma
- Adenoid cystic carcinoma
- Basal cell adenocarcinoma
- Other salivary gland neoplasm

Ancillary Studies:

Immunostains demonstrate tumor cells to be negative for p40; CD117 shows patchy nonspecific expression; CK7 and SOX10 are diffusely positive.

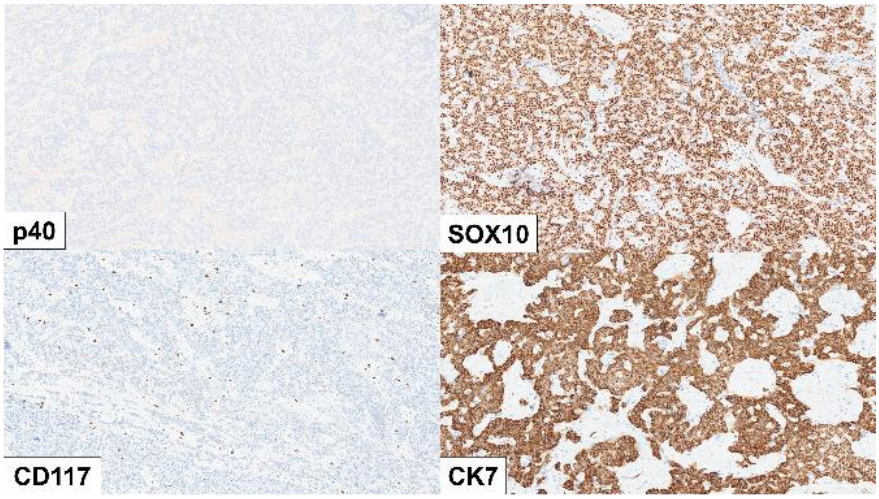

Molecular Testing:

HMGA2::WIF1 fusion was identified on RNA sequencing from the original FNA biopsy.

Pathogenic Findings: *HMGA2::WIF1* Fusion (see Investigative Findings)

Investigative Findings:

Analysis of sequencing data collected for genes beyond the reported subset shows evidence for the presence of a HMGA2::WIF1 fusion in this specimen. This fusion involves a connection between exon 8 of HMGA2 (NM_003484) and exon 8 of WIF1 (NM_007191). The reading frame at the junction point is not straightforward to assess due to the observation of additional splice alterations downstream within WIF1. HMGA2::WIF1 fusions are seen in salivary pleomorphic adenomas with prominent trabecular (canalicular adenoma-like) morphology (PMID: 34324456). As described below, this finding is not validated for clinical decision-making, and should be integrated with other clinical-pathologic data. Follow-up testing using a validated assay may be indicated.

Discussion:

We present a basaloid salivary gland neoplasm that was found to be monophasic and p40-negative on final surgical pathology. Our differential diagnoses includes all basaloid salivary gland neoplasm which are all biphasic and p40-positive. Interestingly, this salivary neoplasm was found to be associated with an *HMGA2::WIF1* fusion on RNA sequencing. Therefore, our favored diagnosis is a new salivary gland neoplasm which we called *HMGA2::WIF1*-associated monophasic salivary neoplasm. This recently-described fusion is present in a subset of basaloid, monophasic salivary neoplasms with canalicular-like morphology and variable behavior (from indolent (adenoma) to infiltrative and recurrent (carcinoma)) (3-6).

In the literature, this entity most commonly manifests in women more than men, 65 year olds, and tend to occur in major salivary glands. Clinically, it has been associated with recurrence and carcinomatous transformation. Approximately 20% of these salivary gland neoplasms have showed malignancy and adverse outcomes (recurrence, distant metastasis, and disease-specific mortality). The most common histological pattern of this tumor has been described as canalicular adenoma-like which shows a monotonous cellular proliferation arranged as trabeculae or canaliculi lined with monolayered, bilayered, or multilayered epithelium. Cytologically, the cells can look oncocytic with abundant eosinophilic cytoplasm, centrally located nuclei, small distinct nuclei and a suggestion of basal striation, resembling native striated ducts, or cuboidal cells with or without spindling with scanty cytoplasm as well as stroma between the canaliculi/trabeculae that is hypocellular, presenting as edematous, hyalinized or myxoid.

The tumor has been shown to be S100 and CK7 positive with rare to focal expression of calponin and p63 in the canalicular-adenoma-like areas. Most importantly, p40 is negative in tumor cells.

This case illustrates the challenge of overlapping cytologic features of basaloid salivary gland neoplasm in a fine needle aspirate. In these cases, the detection of diagnostic fusions with molecular testing is essential for establishing a correct diagnosis. Additionally, the cytologic morphology and definite subclassification of *HMGA2::WIF1*-associated salivary neoplasms is still not fully established.

References:

1. Edmund S. Cibas, Barbara S. Ducatman. Cytology E-Book : Diagnostic Principles and Clinical Correlates. Fourth edition. Saunders; 2014. Accessed November 13, 2025. https://research-ebsco-com.proxy.uchicago.edu/linkprocessor/plink?id=f2021ea6-7d9a-3a5e-9505-d292a5e58554
2. Alsugair Z, Lépine C, Descotes F, et al. Beneath HMGA2 alterations in pleomorphic adenomas: Pathological, immunohistochemical, and molecular insights. Hum Pathol. 2024;152:105633. doi:10.1016/j.humpath.2024.105633
3. Katabi N, Sukhadia P, DiNapoli SE, et al. Expanding the histological spectrum of salivary gland neoplasms with HMGA2::WIF1 fusion emphasising their malignant potential: a report of eight cases. Histopathology. 2024;84(2):387-398. doi:10.1111/his.15074
4. Klubíčková N, Loghides F, van den Hout MFCM, et al. Expanding the Molecular-genetic Spectrum of Canalicular Adenoma-like Subtype of Pleomorphic Adenoma of Salivary Glands. *Am J Surg Pathol*. 2025;49(6):554-563. doi:10.1097/PAS.0000000000002377
5. Dababneh MN, Azzato EM, Nakitandwe J, Cracolici V, Shah AA. HMGA2-positive salivary gland neoplasms with prominent trabecular/canalicular morphology: a focus on carcinomas arising within this phenotype. *Histopathology*. 2025;86(3):385-396. doi:10.1111/his.15334
6. Agaimy A, Ihrler S, Baněčková M, et al. HMGA2-WIF1 Rearrangements Characterize a Distinctive Subset of Salivary Pleomorphic Adenomas With Prominent Trabecular (Canalicular Adenoma-like) Morphology. *Am J Surg Pathol*. 2022;46(2):190-199. doi:10.1097/PAS.0000000000001783

Case 4: Drs. Ellen Willhoit and Aliya Husain

Diagnosis: Pulmonary alveolar microlithiasis

Clinical history: The patient is a 34-year-old male with past medical history significant for interstitial lung disease originally diagnosed in 2021 and subsequent development of chronic hypoxemic respiratory failure. It is suspected that the patient developed the disease long before initial diagnosis due to family history and personal history of chronic respiratory failure. Notably, the patient reported that his mother and brother were also diagnosed with interstitial lung disease, although, the age of diagnosis is unknown. At the time of presentation to UCMC, the patient's supplemental oxygen requirements were 6 liters at rest and 8 liters with activity. Imaging studies (CT and XR) demonstrated diffuse ground-glass opacities, interstitial septal line thickening, paraseptal cystic change, multifocal micro-calfications, and a classic "sandstorm" appearance. The patient received notice of compatible donor lungs, and he presented for bilateral lung transplantation.

Gross examination: The explanted lungs were pink-red and focally hemorrhagic with a pleural surface that was largely smooth and glistening. On palpation, there were patchy areas demonstrating a subtle bumpy texture. Cut surface revealed a fine and gritty texture present diffusely in both right and left lungs.

Microscopic findings: On histologic examination, the major finding was the diffuse presence of numerous round to ovoid, densely purple, and concentric microliths exclusively involving alveolar spaces. Additionally, there was patchy interstitial fibrosis

seen throughout submitted sections, and associated with this interstitial fibrosis was dense chronic inflammatory infiltrates. Approximately two foci of ossification were identified in submitted sections.

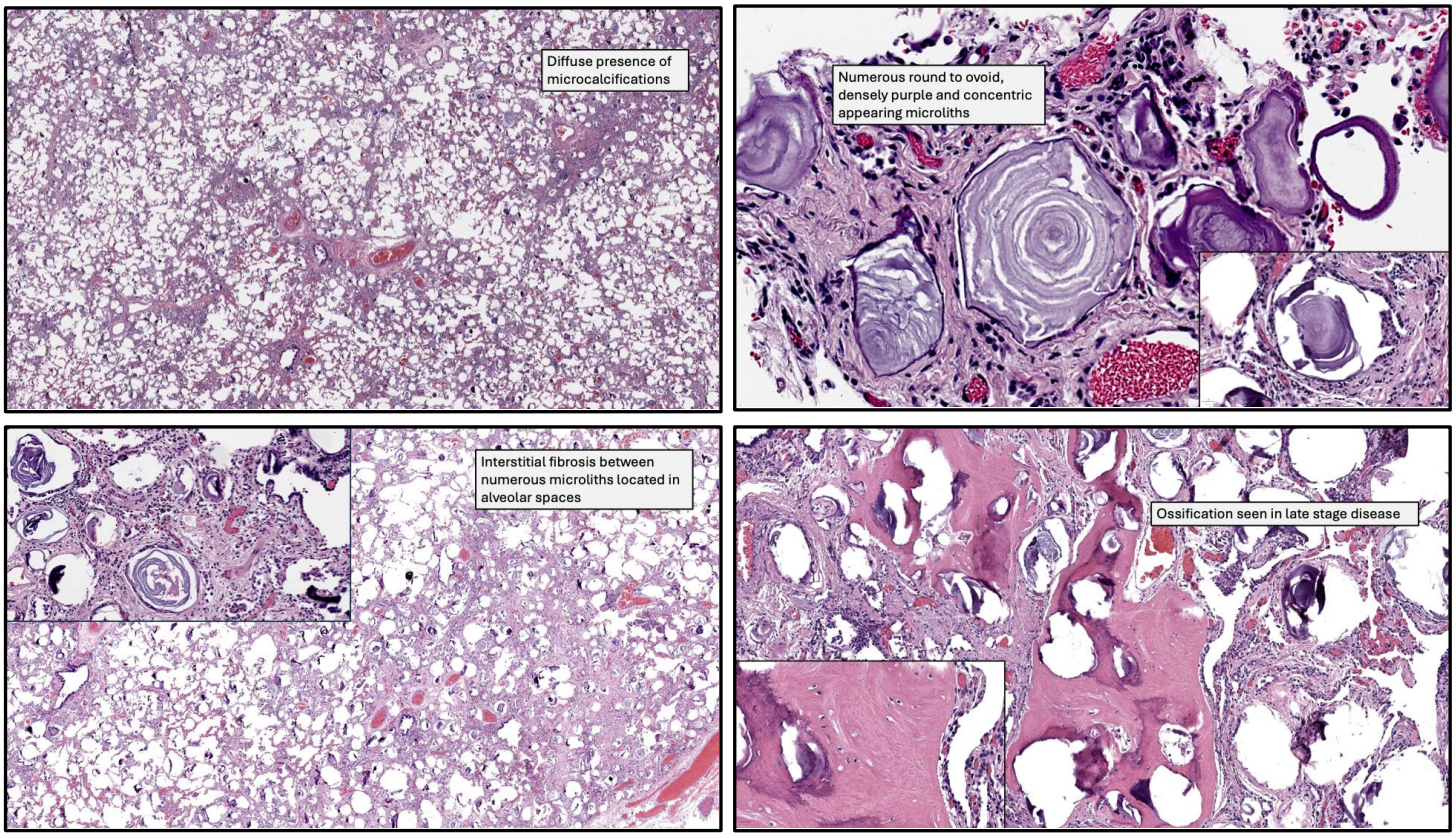

Differential diagnosis:

- Pulmonary alveolar microlithiasis
- Pulmonary alveolar hemosiderosis
- Pulmonary alveolar proteinosis
- Metastatic calcification in chronic renal failure

Final diagnosis: Pulmonary alveolar microlithiasis

Patient follow-up: 4 months post bilateral lung transplantation, the patient has had no exacerbations, cough, or hospitalizations, and he has no supplemental oxygen requirements. Notably, no genetic testing has been performed. On transbronchial biopsy, the lung parenchyma demonstrated no acute cellular rejection or the presence of microliths.

Discussion: Pulmonary alveolar microlithiasis (PAM) is a rare autosomal recessive disorder that causes deposition of innumerable calcium-phosphate crystals (microliths) exclusively in alveolar spaces. PAM is classified as an interstitial lung disease due to the deposition of microliths leading to alveolar/parenchymal damage, and subsequent development of interstitial fibrosis and associated inflammation. Approximately 1,100 cases of PAM have been reported globally from nearly every continent, with the largest number of case reports coming from Turkey, Italy, and the United States. Literature reports a slight male predominance worldwide (50.2%), and it is typically diagnosed in the second and fourth decades of life. In this case, the patient is a 34-year-old male. Sporadic cases have been reported.

Clinical symptoms vary from patient to patient; however, patients are often asymptomatic at the time of diagnosis. If symptomatic, patients usually present with dyspnea on exertion, chronic cough, chest pain, and at times, hemoptysis. Cor pulmonale and chronic hypoxemic respiratory failure are often seen in late-stage disease. There is a key clinical and radiologic disparity seen in PAM. While patients are often asymptomatic or exhibit mild symptoms at diagnosis, when imaging is done at the time of diagnosis, the classic "sandstorm" appearance is already visible.

The deposition of innumerable microliths is due to defective reabsorption of phosphate from alveolar spaces. Underlying mutations leading to loss-of-function are found in the *SLC34A2* gene with the most common variant being a single nucleotide biallelic change. The *SLC34* gene encodes for a sodium-phosphate carrier protein family that consists of type IIa, IIb, and IIc carrier proteins. Type IIa and IIc are primarily located in the proximal tubules of the kidneys. The type IIb carrier protein is expressed in the lungs, intestines, mammary glands, salivary glands, and testes with the primary location being the lungs. The SLC34 cotransporter family is essential in phosphate homeostasis. In the lungs, the type IIb carrier protein is found on the apical membrane of type II alveolar cells, and is responsible for the uptake of phosphate from alveolar fluid. In pulmonary alveolar microlithiasis, the type IIb cotransporter is defective, leading to the accumulation of calcium and phosphate crystals. This defect ultimately results in the deposition of the microliths observed in PAM.

Staging based on imaging findings has been proposed for PAM. In stage 1, the burden of microliths is low. Stage 1 is rarely seen, as most cases have more widespread disease at the time of diagnosis. In stage 2, the classic "sandstorm" appearance is present. At this stage, an abundance of microliths is present, often predominating in the middle and lower lung zones. The boundaries of the heart and diaphragm remain visible. Stage 3 demonstrates the diffuse presence of microliths with loss of heart and diaphragm boundaries. Notably, early stages of interstitial fibrosis are observed. By stage 4, there is

extensive interstitial calcification and pleural involvement with prominent interstitial fibrosis, microcysts, and beginning ossification. Based on these findings, the patient in this case likely presented during late stage 4 disease.

Currently, treatment is supportive in nature prior to lung transplantation. Supportive measures include oxygen supplementation, appropriate vaccinations, and abstaining from smoking. Bisphosphonate therapy been reported in 12 cases of PAM, but the results varied and did not support bisphosphonates as an effective therapeutic option. There is no definitive treatment; however, single and bilateral lung transplantations have shown promise. Approximately 12 transplantations in the setting of PAM have been reported, and thus far, no known recurrences have occurred in both single and bilateral transplants. Ultimately, the prognosis for PAM is severe because patients will eventually experience respiratory failure and often have secondary cardiac involvement usually due to pulmonary hypertension. Until less invasive and effective treatments are discovered, transplantation is needed for treatment of the disease.

References:

1. Bell, Daniel, and Yuranga Weerakkody. "Pulmonary Alveolar Microlithiasis." *Radiopaedia.org*, Mar. 2010, https://doi.org/10.53347/rid-8842.
2. Castellana, Giuseppe, et al. "Pulmonary Alveolar Microlithiasis: Review of the 1022 Cases Reported Worldwide." *European Respiratory Review*, vol. 24, no. 138, Nov. 2015, pp. 607–20. https://doi.org/10.1183/16000617.0036-2015.
3. Enemark, Asbjørn, et al. *Pulmonary Alveolar Microlithiasis – a Review*. 29 Dec. 2021, pmc.ncbi.nlm.nih.gov/articles/PMC8686773
4. Jönsson, Åsa Lina M., et al. "New Insights in the Genetic Variant Spectrum of SLC34A2 in Pulmonary Alveolar Microlithiasis; a Systematic Review." *Orphanet Journal of Rare Diseases*, vol. 18, no. 1, May 2023, p. 130. https://doi.org/10.1186/s13023-023-02712-7.
5. Kashyap, Surender, and PrasantaR Mohapatra. "Pulmonary Alveolar Microlithiasis." *Lung India*, vol. 30, no. 2, Jan. 2013, p. 143. https://doi.org/10.4103/0970-2113.110424.
6. Khaladkar, Sanjay Mhalasakant, et al. "Pulmonary Alveolar Microlithiasis - Clinico-Radiological Dissociation - a Case Report With Radiological Review." *Journal of Radiology Case Reports*, vol. 10, no. 1, Jan. 2016, pp. 14–21. https://doi.org/10.3941/jrcr.v10i1.2528.
7. Klikovits, Thomas, et al. "A Rare Indication for Lung Transplantation – Pulmonary Alveolar Microlithiasis: Institutional Experience of Five Consecutive Cases." *Clinical Transplantation*, vol. 30, no. 4, Feb. 2016, pp. 429–34. https://doi.org/10.1111/ctr.12705.

8. Kosciuk, Patrick, et al. “Pulmonary Alveolar Microlithiasis.” *European Respiratory Review*, vol. 29, no. 158, Nov. 2020, p. 200024. https://doi.org/10.1183/16000617.0024-2020.
9. Mardani, Parviz, et al. “Successful Bilateral Lung Transplantation in Pulmonary Alveolar Microlithiasis: A Case Report and Review of Literature.” *The Clinical Respiratory Journal*, vol. 18, no. 5, May 2024, p. e13773. https://doi.org/10.1111/crj.13773.
10. Traebert, Martin, et al. “Expression of Type II Na-Picotransporter in Alveolar Type II Cells.” *American Journal of Physiology-Lung Cellular and Molecular Physiology*, vol. 277, no. 5, Nov. 1999, pp. L868–73. https://doi.org/10.1152/ajplung.1999.277.5.l868.

Case 5: Drs. Sharanpreet Hira, Tatjana Antic, and Nicole Cipriani

Diagnosis: Metastatic carcinoma with *DEK::AFF2* fusion

Clinical history: The patient is a 75-year-old with a history of ulcerative colitis on mesalamine and type 2 diabetes, who presented with a 2.2 cm left medial canthal mass that was progressively increasing in size. The mass was believed to be a stye, however, after no improvement with heat compress, the patient went to see his dermatologist. A biopsy was performed at that time. The patient underwent orbitotomy and radiation. Subsequently, the patient noticed a small mass in the left tail of the parotid region. The patient underwent excision.

Gross Findings (on parotid resection specimen):

The lesion is a 1.2 cm mass, white–tan, nodular, unencapsulated and circumscribed. Appears to abut the inked resection margin in some of the slices.

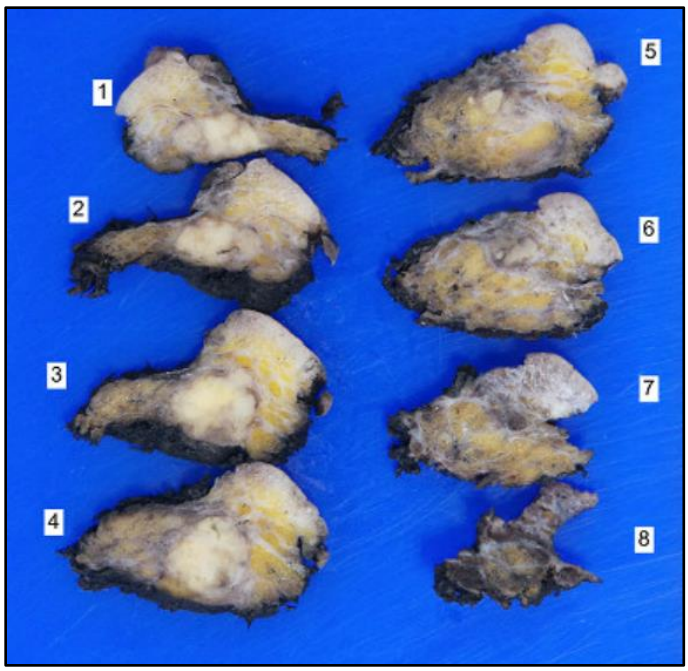

Microscopic findings (on excision): The tumor is unencapsulated, well-circumscribed arranged in nests and sheets. On higher power, these nests and sheets of cells show a focal keratin pearls and a neutrophilic infiltrate tends to be in between the tumor cords or nests. There are occasional signet ring like cells with focal neutrophilic micro-abscesses, with a focal cribriform pattern.

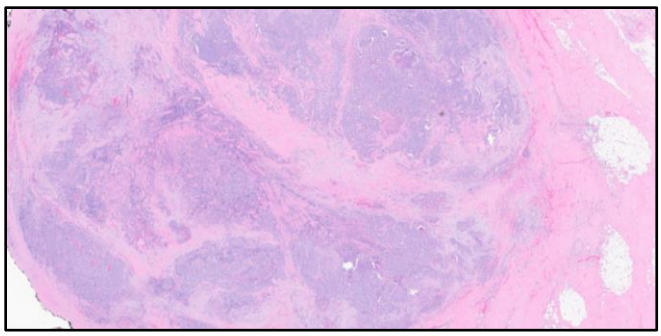

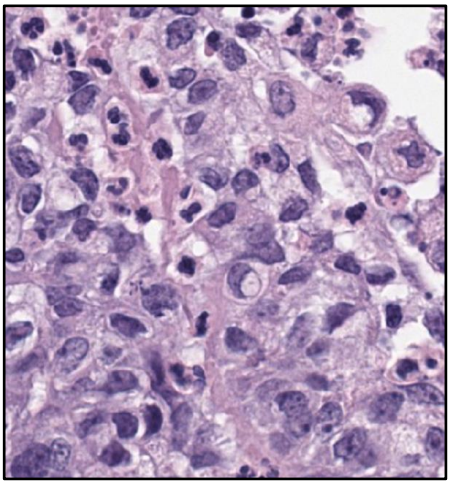

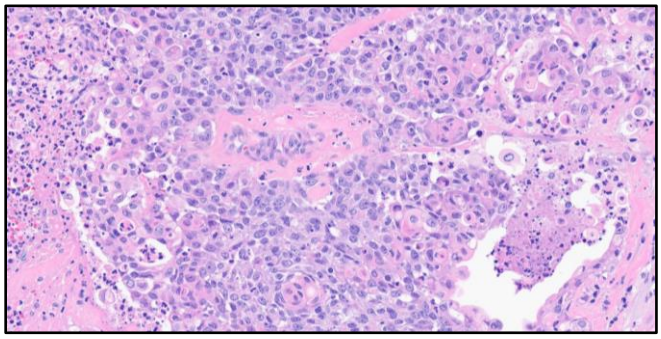

Differential Diagnosis:

- **Primary salivary gland tumors**
  - High grade mucoepidermoid carcinoma
  - High grade salivary duct carcinoma
- **Metastatic/secondary tumors**
  - Squamous cell carcinoma
  - NUT carcinoma

Ancillary Studies:

The tumor was positive within the malignant cells for the following immunohistochemical studies: diffusely positive for CK7, mostly positive for p40, and negative for S100. PD-L1 immunohistochemical stain is negative. Controls are appropriate. The original lacrimal gland excision showed the malignant cells to be positive for p63 and patchy CK5/6. The original lacrimal gland excision showed the malignant cells to be negative for p16, synaptophysin, and chromogranin.

Molecular Testing:

A DNA based NGS panel was performed that demonstrated no pathogenic findings. However, the RNA-based sequencing demonstrated a DEK::AFF2 fusion. The fusion involves a connection between exon 7 of DEK (NM_003472) and exon 4 of AFF2 (NM_002025), and it appears to retain the proper reading frame at the junction point.

Discussion:

We are presented with a metastatic carcinoma that is positive for p40, CK-7 and negative for S100. Our favored diagnosed is metastatic carcinoma with a *DEK::*AFF2 fusion which is a rare entity in the literature that most commonly presents as sinonasal and skull based tumors.

It typically displays a complex endophytic and exophytic, frequently papilloma-like growth with a transitional epithelium with eosinophilic to amphophilic cytoplasm. There is absent or minimal keratinization with occasional compact keratin pearls. The neutrophilic infiltrate tends to be in between the tumor cords or nests with less intra-epithelial infiltrate. When compared to conventional squamous cell carcinoma, it lacks cellular atypia and frequent pleomorphism.

This case illustrates that carcinomas with relatively bland morphology can be a distinct entity with a key *DEK::AFF2* fusion. *DEK::AFF2* carcinomas showed frequent local recurrence, cervical lymph node metastases, and distant metastasis, despite relatively bland histology. This tumor merits increased pathologic recognition to better understand its prognostic and therapeutic implications.

References:

1. WHO Blue Book Online

2. Expertpath

3. College of American Pathologists Cancer Protocols

4. Kuo YJ, Lewis JS Jr, Zhai C, Chen YA, Chernock RD, Hsieh MS, Lan MY, Lee CK, Weinreb I, Hang JF. DEK-AFF2 fusion-associated papillary squamous cell carcinoma of the sinonasal tract: clinicopathologic characterization of seven cases with deceptively bland morphology. Mod Pathol. 2021 Oct;34(10):1820-1830. doi: 10.1038/s41379-021-00846-2. Epub 2021 Jun 9. PMID: 34108636.5. Kao, Jsun-Liang et al. “Rare anaplastic sarcoma of the kidney: A case report.” *World journal of clinical cases* vol. 8,8 (2020): 1495-1501. doi:10.12998/wjcc.v8.i8.1495

5.. Rooper LM, Agaimy A, Dickson BC, Dueber JC, Eberhart CG, Gagan J, Hartmann A, Khararjian A, London NR, MacMillan CM, Palsgrove DN, Nix JS, Sandison A, Stoehr R, Truong T, Weinreb I, Bishop JA. DEK-AFF2 Carcinoma of the Sinonasal Region and Skull Base: Detailed Clinicopathologic Characterization of a Distinctive Entity. Am J Surg Pathol. 2021 Dec 1;45(12):1682-1693. doi: 10.1097/PAS.0000000000001741. PMID: 34049316.7.

6. Owosho AA, Gleysteen JP, Wood CB, Franklin A, Angel J, Jain R. *DEK::AFF2* Squamous Cell Carcinomas of the Sinonasal Region and Temporal Bone Diagnosed After Recurrences: A Report of Two Patients. Int J Surg Pathol. 2025 Aug;33(5):1258-1266. doi: 10.1177/10668969241301061. Epub 2025 Jan 17. PMID: 39819065.

Case 6: Drs. Hermon Kihshen, Hayley Zullow and Tatjana Antic

Diagnosis: ALK-rearranged renal cell carcinoma

Clinical History: A 61-year-old woman with a history of hypertension and chronic kidney disease presented with gross hematuria and was found to have a solid mass in the upper pole of the right kidney on US. CT abdomen and pelvis demonstrated that the mass was in continuity with the right renal pelvis and proximal ureter. As a result, the renal mass was favored to be of urothelial origin. The patient subsequently underwent right nephroureterectomy which revealed a 14.1 x 5.0 x 4.4 cm, well-circumscribed, solid-to-cystic mass that extended grossly into the proximal ureter. The patient had uncomplicated recovery with no evidence of disease recurrence one and a half years later.

Gross Findings (on resection specimen)

Solid and cystic tumor extending into proximal ureter.

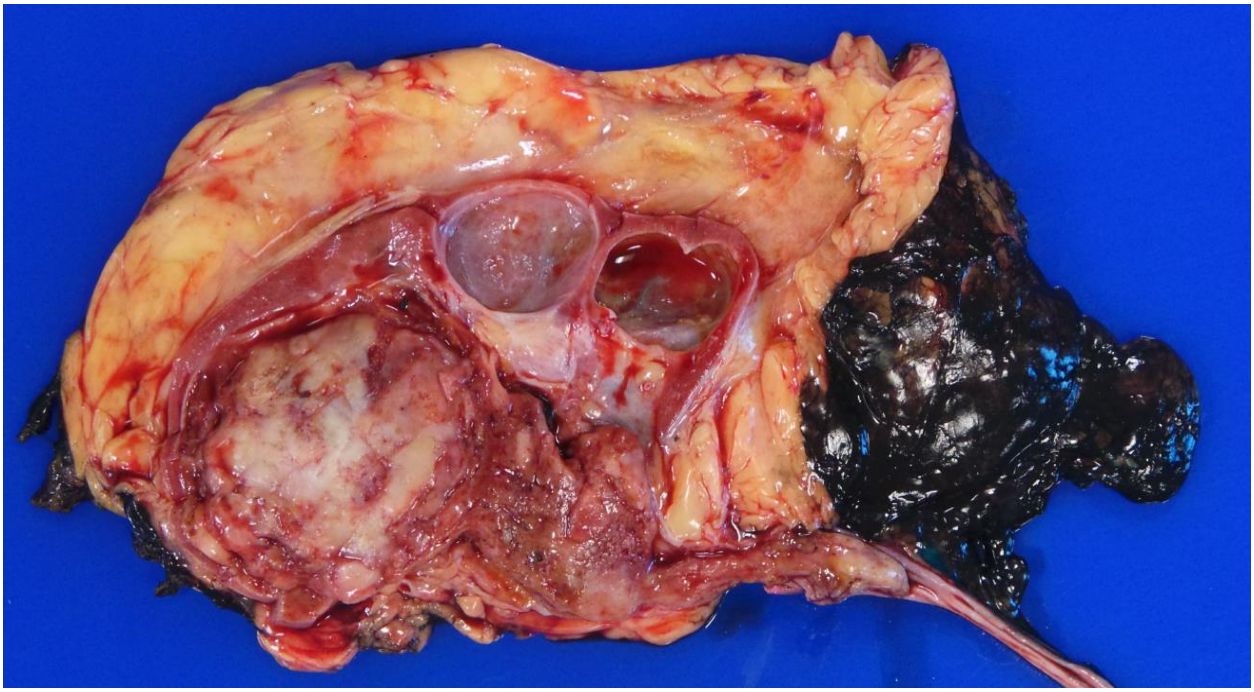

Microscopic findings (on resection specimen):

A.

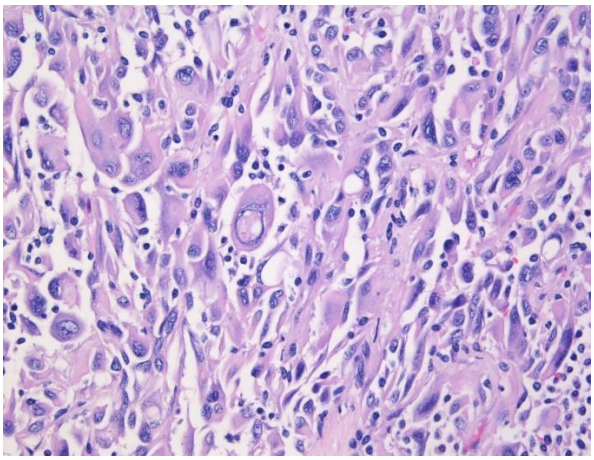

A. This focus shows a mixture of spindle and pleomorphic cells with nuclei of variable size. There are occasional nuclear pseudo-inclusions, multinucleated tumor cells, and inflammatory cells. The cytoplasm is abundant, dense and eosinophilic.

B.

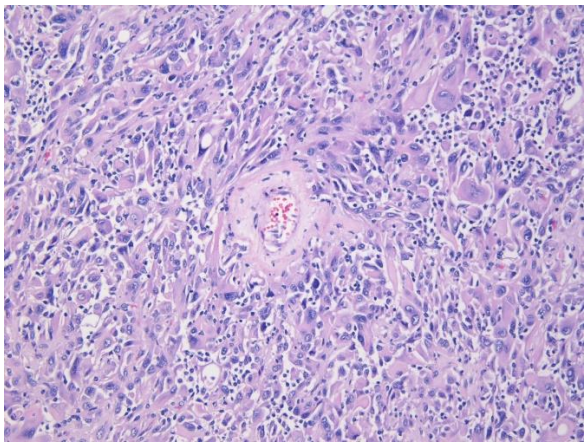

B and C. Other areas of the tumor show malignant cells radiating from the thick vessel wall as well as forming slit like spaces filled with red blood cells.

C.

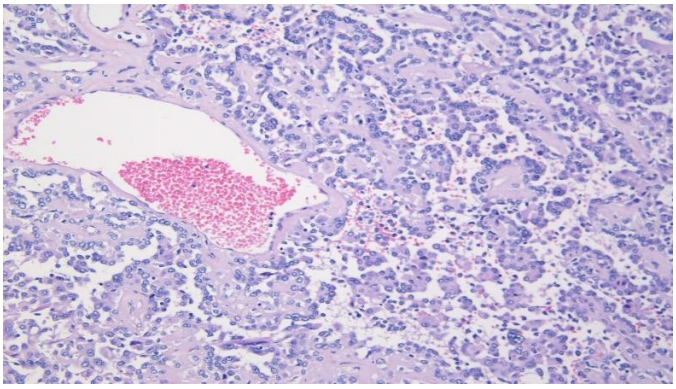

Differential Diagnosis:

- Epithelioid angiomyolipoma
- Epithelioid angiosarcoma
- Sarcomatoid carcinoma (RCC vs. Urothelial)

Ancillary Studies:

Immunohistochemical stains show that the tumor is positive for vimentin, Cam5.2, EMA, PAX8, CK7 (focal), TFE3 (focal), HMB45 and p63 (focal). The tumor is negative for GATA3, ERG, SMA, ALK1 and CK20. INI-1 expression is preserved. PD-L1 is positive in 10% of the malignant cells.

Molecular Testing:

RNA fusion NGS showed the following pathogenic findings: *TPM3::ALK* Fusion.

Discussion:

This case illustrates an ALK-rearranged renal cell carcinoma with a *TPM3::ALK* fusion showing marked pleomorphism, multinucleated giant cells, and a inflammatory cells. The broad differential diagnosis included epithelioid angiomyolipoma, angiosarcoma and sarcomatoid carcinoma of either renal or urothelial origin. These were excluded based on the immunoprofile and molecular studies.

Importantly, ALK immunostaining using the "ALK1" clone was negative, contributing to initial diagnostic uncertainty. Prior reports describe similar false-negative results with this antibody in TPM3::ALK-associated RCC. This highlights a key diagnostic pitfall and highlights the need for more sensitive clones (e.g., D5F3) or molecular testing when ALK-RCC is suspected.

Features seen in this case such as spindle and multinucleated cells, rhabdoid morphology, and presence of inflammatory cells align with previously described *TPM3::ALK*-associated RCC, suggesting that certain architectural and cytologic patterns may correlate with specific ALK fusion partners.

Accurate diagnosis is clinically important due to emerging targeted therapies. ALK inhibitors have demonstrated meaningful responses in metastatic ALK-RCC, and in this case, PD-L1 expression (10%) suggests potential sensitivity to immune checkpoint blockade as well. Therefore, unequivocal identification of ALK rearrangement especially in morphologically unusual renal tumors with atypical immunohistochemical profiles remains essential.

References:

1. Mariño-Enríquez A, Ou WB, Weldon CB, Fletcher JA, Pérez-Atayde AR. ALK rearrangement in sickle cell trait-associated renal medullary carcinoma. Genes Chromosomes Cancer. 2011 Mar;50(3):146-53. doi: 10.1002/gcc.20839. Epub 2010 Dec 13. PMID: 21213368.
2. Debelenko LV, Raimondi SC, Daw N, Shivakumar BR, Huang D, Nelson M, Bridge JA. Renal cell carcinoma with novel VCL-ALK fusion: new representative of ALK-associated tumor spectrum. Mod Pathol. 2011 Mar;24(3):430-42. doi: 10.1038/modpathol.2010.213. Epub 2010 Nov 12. PMID: 21076462.
3. Smith NE, Deyrup AT, Mariño-Enriquez A, Fletcher JA, Bridge JA, Illei PB, Netto GJ, Argani P. VCL-ALK renal cell carcinoma in children with sickle-cell trait: the eighth sickle-cell nephropathy? Am J Surg Pathol. 2014 Jun;38(6):858-63.

doi: 10.1097/PAS.0000000000000179. PMID: 24698962; PMCID: PMC4352307.

4. Kuroda N, Trpkov K, Gao Y, Tretiakova M, Liu YJ, Ulamec M, Takeuchi K, Agaimy A, Przybycin C, Magi-Galluzzi C, Fushimi S, Kojima F, Sibony M, Hang JF, Pan CC, Yilmaz A, Siadat F, Sugawara E, Just PA, Ptakova N, Hes O. ALK rearranged renal cell carcinoma (ALK-RCC): a multi-institutional study of twelve cases with identification of novel partner genes CLIP1, KIF5B and KIAA1217. Mod Pathol. 2020 Dec;33(12):2564-2579. doi: 10.1038/s41379-020-0578-0. Epub 2020 May 28. PMID: 32467651.
5. Galea LA, Hildebrand MS, Witkowski T, Joy C, McEvoy CR, Hanegbi U, Aga A. ALK-rearranged renal cell carcinoma with TPM3::ALK gene fusion and review of the literature. Virchows Arch. 2023 Mar;482(3):625-633. doi: 10.1007/s00428-022-03451-z. Epub 2022 Nov 12. PMID: 36370168.